Electronic Aspects of Propagation in Left-Handed Guided Wave Structures: Electromagnetic-Media Interactions

Clifford M. Krowne and Maurice Daniel*

Microwave Tech. Br., Electronics Tech. Div., Naval Research Laboratory, Wash., D.C. 20375-5347

*DCS Corporation, 1330 Braddock Place, Alexandria, VA 22314

Abstract: **Dispersion diagrams and magnetic and electric field distributions are found for a microstrip structure containing a left-handed medium (LHM). The material constituting the LHM making the substrate has characteristics chosen to overlap with potentially realizable substances. Calculations are done using a fast solver Green's function spectral domain computer code. It is found that the dispersion diagrams and field distributions are very unusual and admit the possibility of completely new device realizations based on combining LHM with conventional materials in a multi-layered configuration.**

I. Introduction

There has been great interest in the last few years in trying to understand the properties of structures configured for making focusing devices capable of having radically new properties based on the concepts coming from the use of what has been variously referred to in the literature as negative media, left-handed media, double negative media, or backward wave media [1]-[12]. There are many unusual properties of such media, and although in the physics and electronics literature many fascinating issues have been explored, we will not address what has held the attention of most researchers, which are the properties leading to convergent focusing behavior [1], [3] when ordinary media would lead to divergent rays and the attendant perfect focusing consequences. All that will be stated is that in light of multi-dimension aspects of real lensing systems, and imperfect media, including finite dispersion and finite loss, the sought after effect may turn out to be not quite what was expected [5], [11], although still tremendously interesting, nevertheless.

Here no less a fascinating aspect of LHM will be explored, the electronic guiding wave properties of structures loaded with such media. We choose to define the LHM medium phenomenologically by assigning to it a negative permittivity $\varepsilon < 0$ and permeability $\mu < 0$, simultaneously satisfied. The slight difference in this definition of a LHM versus say using a backward wave definition, although noticeable, is not enough to confuse the basic phenomenon to follow. Our aim is to first explore the area of dispersion diagram description of a realistic structure for wave propagation, then study some dependencies on the LHM description, and once coming away with some insight of electronic operation, to seek some electromagnetic field plots to elucidate what might be available in the realm of original devices employing a configuration which yields entirely new distributions of fields.

This is a tall order, and we do not want to overstate our aim. It will be sufficient to merely obtain enough results as outlined above to direct the next effort into understanding where LHM may be useful for integrated circuits. Our work will delve into the microwave and millimeter wavelength regimes. It is expected that the use of LHM in electronic microwave and millimeter wave devices will allow new types of phase shifters, couplers, and isolators, for example, to be developed. Below we will first turn our attention to the dispersion diagrams of single microstrip strutcures.

II. Dispersion Diagrams

A single microstrip structure is considered because microstrip is one of the basic building blocks of microwave circuits in electronic integrated circuits. Because nothing is known about the characteristics of multi-layered microstrip structures utilizing LHM's, we will study the most basic configuration, a single substrate case. Figure 1 shows such a structure, which includes the bounding walls (not shown). The strip is presumed perfect metal with width $w = 0.5$ mm. Substrate thickness of the LHM is $h_1 = 0.5$ mm, which makes $h_1 = w$ for this particular configuration. Symmetrically disposed vertical side walls are placed at $x = \pm 2.5$ mm, making the total wall-to-wall separation $b = 5.0$ mm. Second layer above the substrate is selected to be vacuum (ideal air) with thickness $h_2 = 5.0$ mm, making $h_2 = b = 10w = 10h_1$.

US Government Work Not Protected by US Copyright.

Because the absolute values in permittivity $|\varepsilon|$ and permeability $|\mu|$ are nominally in the experimentally frequency band limited range of 1 to 10, we choose $\varepsilon = -2.5$ and permeability $\mu = -2.5$ (relative values) as potentially practical values for which simulations would be demonstrative.

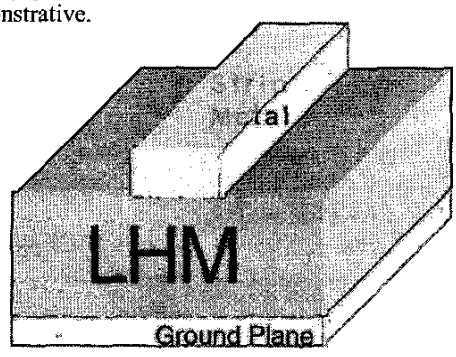

Figure 1
Perspective drawing of the structure to be simulated

Figure 2 shows the dispersion diagram giving propagation constant $\gamma = (\alpha+j\beta)/k_0$, against the frequency f (GHz). Note that the propagation constant is provided in normalized form, a unitless quantity. This calculation has been done using a spectral domain simulation employing the moment method with a general Green's function capable of handling arbitrary anisotropy and non-hermitian media [13]. That is, the tensors describing the materials, in this case the LHM, could in fact be anisotropic and lossy. However, what we have done here is limit ourselves to the situation of isotropy and lossless media, in this case that of the LHM. This will in no way limit our results and insights sought which will rely on the basic aspects of LHM and hermiticity. Vertical dashed lines (red) indicate frequency points at which we will later find field distributions.

For now, direct attention to the upper (blue) curve giving β and the lower (green) curve giving α. Below 6 GHz and above 75 GHz only β is nonzero. In these regions, therefore, due to $\alpha = 0$, pure propagation of the wave will occur down the guiding structure, call it z for the structure. This is not the case for the intermediate region $6 < f < 75$ GHz. Here $\alpha > 0$, causing the wave to evanesce, a property of a wave traveling which can occur in a medium with a hermitian constitutive tensor. Examination of the area close to $f = 0$ shows that the slope of $d\beta/df$ becomes gentle while being positive. Thus one can identify the whole dispersion curve as being associated with a fundamental mode, not unlike that seen for ordinary media substrates which would limit to a finite β value as $f \rightarrow 0$. Of course, this limiting value is a characteristic of guiding structures with central metal pieces not touching the bounding perfect electric walls.

These bounding electric walls are similar to those found in enclosed structures, and here are, in fact, what may be referred to as computational walls.

Phase velocity is given by $v_p = \omega/\beta = 2\pi f/\beta$, and this can be seen to be positive for the entire plotted dispersion curve β. But the story is different for the group velocity $v_g = d\omega/d\beta = 2\pi df/d\beta = 2\pi/[d\beta/df]$. For the region $6 < f < 26$ GHz, the quantity $d\beta/df < 0$, making $v_g < 0$ while $v_p > 0$, which is to say that with respect to propagation in the z-direction, the wave is a backward wave. Likewise, in the region where $f > 75$ GHz, for the lower branch, again $d\beta/df < 0$, giving us a backward wave in the region where pure phase propagation occurs. This backward wave behavior does not occur in the low frequency regime, however, nor in the upper branch beyond $f = 75$ GHz.

A backward wave will have the power, or energy flow per unit time, in the opposite direction than the phase propagation [2], [10]. Since the variation of the harmonic spectral solution has a time and z-dependence like $e^{i\omega t-\gamma z}$, which is equal to $e^{i(\omega t-\beta z)}e^{-\alpha z}$, the vector product $\mathbf{v}_{pl} \cdot \mathbf{v}_{gl}$ sign determines whether or not the wave is backward or not. If $\mathbf{v}_{pl} \cdot \mathbf{v}_{gl} < 0$, the the wave is backward. Notice also for the waves, that $\alpha > 0$, assuring us that casuality is satisfied. The backwardness of the wave in the transmission (longitudinal) direction z should not be confused with the inherent backwardness (or nearly, so with the earlier caveat) of the LHM. This inherent wave backwardness displays itself by acting in the propagation phase $\mathbf{v}_{pt}$ and group $\mathbf{v}_{gt}$ transverse velocities in the xy cross-section as they constructively and destructively interfere when waves enter the LHM.

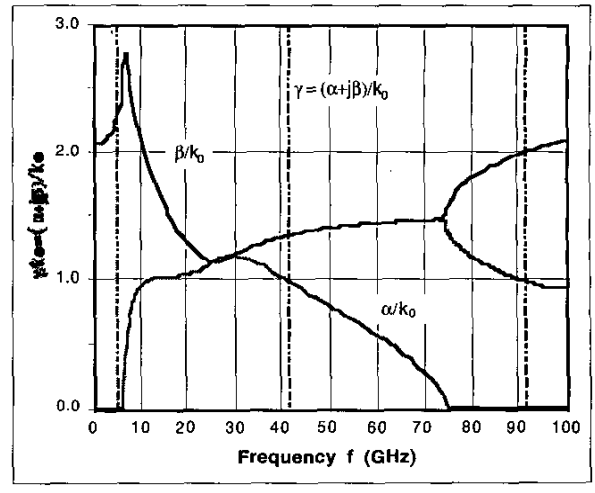

Figure 2
Dispersion diagram for a single microstrip with LHM

A word should be said about other modal solutions. As the frequency gets higher, generally speaking, more modes seem to become admissible. This is not surprising, and not unlike what we are familiar with for ordinary media. Thus, in the higher frequency regime,

around 80 GHz, for example, the cluttering of the modal spectrum on a dispersion diagram plot arises. We have purposely left this out in order not to confuse the discussion. Numerical calculations were done using $n_x = n_z = 1$ basis expansion functions for the driving currents on the strip in the x and z-directions, where the x-direction is in the horizontal direction, the y-coordinate normal to the plane of the layers. Tests were done also for using $n_x = n_z = 5$ and 9. The spectral sum operator in the Fourier transform domain $\sum_{-n_{max}}^{n_{max}}$, has $n_{max} = 200$ although it too has been looked at for higher $n_{max} = 400$. Only tiny dependencies were seen on these numerical parameters.

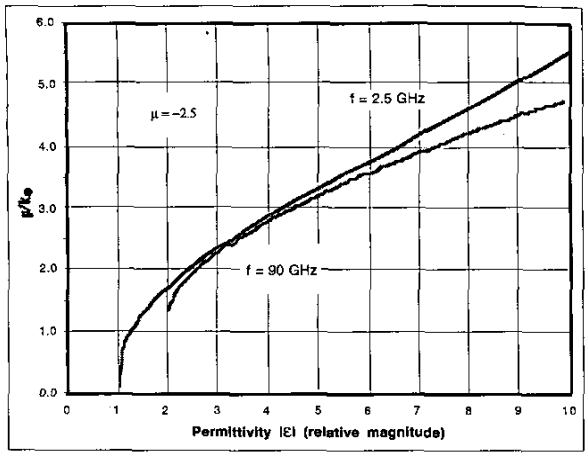

Figure 3
Phase versus LHM permittivity variation

Figure 3 gives the variation of the phase propagation constant β against the absolute value $|\varepsilon| = -\varepsilon$ of the permittivity. This has been done for two frequencies, each in the regions of pure propagation, f = 2.5 GHz and 90 GHz. For small $|\varepsilon|$, the increase is exponential, but it rapidly slows to a linear trend for the upper f = 2.5 GHz (magenta) curve, and a sub-linear trend for the lower f = 90 GHz (green) curve. The upper curve provides β over a 10:1 range of permittivity, whilst the lower curve does this nearly over a 5:1 range.

Next we will turn our attention to the electromagnetic field distributions in the following section.

III. Electromagnetic Fields

Once the propagation constant is found, the expansion coefficients used in the driving strip currents may be calculated. And with this determination, the electromagnetic fields are then found too. Since the processing occurs in the spectral domain, the final fields must be mapped back into the real space domain, allowing field distributions to be produced. Figure 4 shows both the magnetic field magnitude H and the cross-sectional vector field $\mathbf{H}_t$, which with the longitudinal field component H_z generates the total vector field in 3D, $\mathbf{H} = \mathbf{H}_t + H_z\mathbf{z}$ where $\mathbf{z}$ is the unit vector in the z-direction and $\mathbf{H}_t = H_x\mathbf{x} + H_y\mathbf{y}$. The plotted H magnitude distribution in Fig. 4 is not the cross-sectional magnitude using only the cross-sectional components of $\mathbf{H}$, but rather the full vector.

All field plots below are generated from a uniform 8372 square grid from the spectral domain code, from which a plotting package Fortner is used to interpolate for E or H, or produce a 22×23 or 23×23 grid for $\mathbf{H}_t$ or $\mathbf{E}_t$. Grid overlays are done by maintaining bilateral symmetry with respect to the y-axis for $\pm$ x. (This is why we have ended up with two closely spaced vertical left figure bounding walls, merely an artifact.)

The overall trend of the magnetic field is to have clockwise circulation in the LHM substrate, and reverse or counterclockwise circulation in the overlying region. There are also more local vector field behaviors on a square grid by square grid basis, which display local circulation behaviors and interfacial normal and tangential field continuity consistent with the difference in media. Evidence of the unusual interfacial field effects are especially apparent just to the right and left of the strip metal (located at x = $\pm$ 0.25 mm) and continuing to the

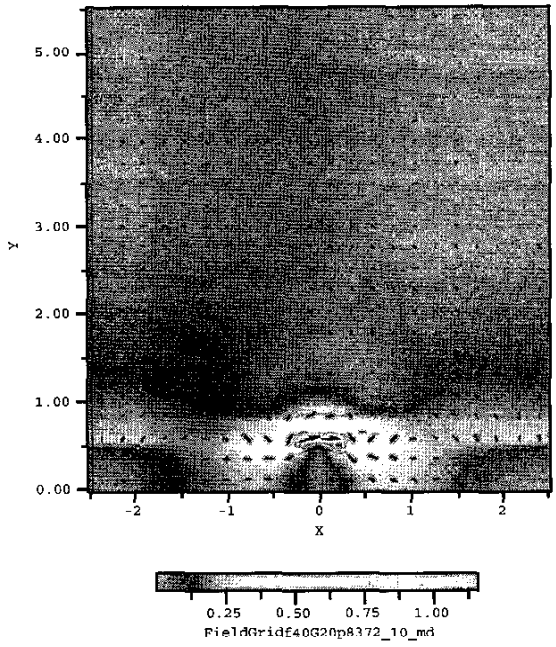

Figure 4
Magnetic field magnitude H and vector $\mathbf{H}$ at 40 GHz

side walls, where the sign switch in the normal components occurs necessitated by continuous H_x and

continuous B_y requirements. Sign switch is imposed by B_y since it is scaled from H_x by the constitutive scalar μ. Similar to Fig. 4, Fig. 5 shows the electric field magnitude E and the cross-sectional vector field $\mathbf{E}_t$. Again there are local vector field behaviors, which display

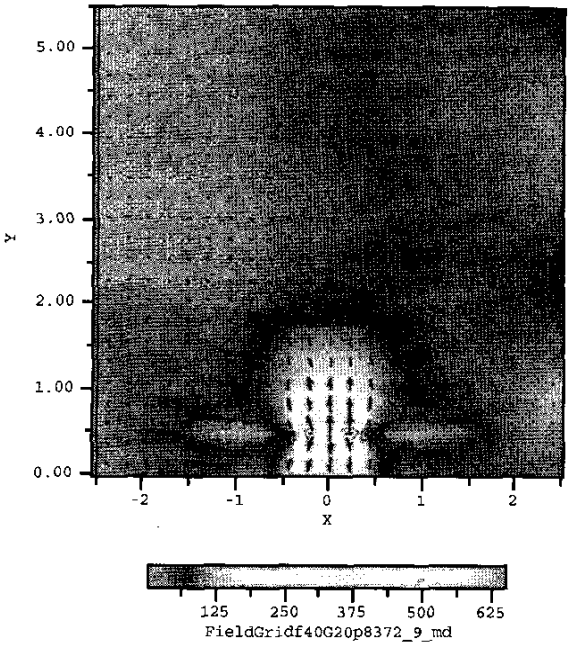

Figure5
Electric field magnitude E and vector **E** at 40 GHz

local directional behaviors and interfacial normal and tangential field continuity consistent with the difference in media. Evidence of the unusual interfacial field effects are seen due to the sign switch in the normal component occurring as necessitated by continuous E_x and continuous D_y requirements. Sign switch is imposed by D_y since it is scaled from E_x by the constitutive scalar ε.

Field distributions have been calculated at 5 and 90 GHz also, but space does not enable us to show them here. What is learned from all these electromagnetic field distributions, is that the disposition of the fields are radically different from that seen when ordinary media substrates are employed. Although not entirely unexpected, what is surprising are the specific attributes caused by utilizing LHM.

VII. Conclusion

Here we have determined the dispersion diagrams for a microstrip structure loaded with left-handed media. These diagrams are quite unlike that for ordinary substrates, and open up the possibility of designing entirely new electronic devices. Further support and understanding comes with determining the electromagnetic field distributions, and we have shown some here. There are still other ways of displaying the electromagnetic behavior in distributions (not shown here), and we have been exploring these in order to ascertain the surprising and sometimes astonishing characteristics of guided wave structures employing LHM. This area of research is just in its infancy in terms of looking at what such materials could do for microwave and millimeter wave integrated circuits, and we expect, many more interesting results to follow.

References

[1] R. W. Ziolkowski & S. Heyman, "Wave propagation in media having negative permittivity and permeability," Phys. Rev. E, vol. 64, pp. 056625-1 to 15, 2001.

[2] I. V. Lindell, S. A. Tretyakov, K. I. Nikoskinen & S. Ilvonen "BW media - media with negative parameters, capable of supporting backward waves," Microwave & Optical Tech. Letts., vol. 31, pp. 129 - 133, Oct. 20, 2001.

[3] C. Luo, S. G. Johnson & J. D. Joannopoulos, "All-angle negative refraction in a three-dimensionally periodic photonic crystal," Appl. Phys. Letts., vol. 81, pp. 2352 - 2354, Sept. 23, 2002.

[4] D.R. Fredkin and A. Ron, "Effectively left-handed (negative index) composite material," Appl. Phys. Letts., vol. 81, pp. 1753 - 1755, Sept. 2, 2002.

[5] R. M. Walser, A. P. Valanu & P. M. Valanju, "Comment on 'Extremely low frequency plasmons in metallic mesostructures,'" Phys. Rev. Letts., vol 87, p. 119701-1, Sept. 10, 2001.

[6] M. Notomi, "Theory of light propagation in strongly modulated photonic crystals: refractionlike behavior in the vicinity of the photonic band gap," Phys. Rev. B, vol. 62, pp. 10696-10705, Oct. 15, 2000.

[7] D. R. Smith, D. C. Vier, W. Padilla, S. C. Nemat-Nasser & S. Schultz, "Loop-wire medium for investigating plasmons at microwave frequencies," Appl. Phys. Letts., vol. 75, pp. 1425-1427 Sept. 6, 1999.

[8] D. R. Smith, S. Schultz, N. Kroll, M. Sigalas, K. M. Ho, & C. M. Soukoulis, "Experimental and theoretical results for a two-dimensional metal photonic band-gap cavity," Appl. Phys. Letts., vol 65, pp. 645-647, Aug. 1, 1994.

[9] J. Gerardin & A. Lakhtakia, "Negative index of refraction and distributed bragg reflectors, " Microwave & Optical Tech. Letts., vol 34, pp. 409-411, Sept. 20, 2002.

[10] M. W. McCall, A. Lakhtakia & W. S. Weiglhofer, "The negative index of refraction demystified, " European J. Phys., vol. 23, pp. 353-359, 2002.

[11] A. L. Pokrovsky & A. L. Efros, "Electrodynamics of metallic photonic crystals and the problem of left-handed materials," Phys. Rev. Letts., vol. 89, pp. 093901-1 to 4, Aug. 26, 2002.

[12] A. Lakhtakia, "An electromagnetic trinity from negative permittivity & negative permeability," Intern. J. Infrared & Millimeter Waves, vol. 23, pp. 813-818, June 2002.

[13] C. M. Krowne, "Dyadic Green's function modifications for obtaining attenuation in microstrip transmission layered structures with complex media," IEEE Trans. Microwave Th. & Tech., vol. 50, pp. 112-122, Jan. 2002.